Distribution of Fano parameters in a mesoscopic system with broken time-reversal symmetry

2007 J. Phys. A: Math. Theor. 40 5857

(http://iopscience.iop.org/1751-8121/40/22/006)

IOP Publishing Journal of Physics A: Mathematical and Theoretical

J. Phys. A: Math. Theor. **40** (2007) 5857–5864 doi:10.1088/1751-8113/40/22/006

Distribution of Fano parameters in a mesoscopic system with broken time-reversal symmetry

V Uski[1,3], F Mota-Furtado[2] and P F O'Mahony[2]

[1] Department of Physics, University of Turku, 20014 Turku, Finland
[2] Department of Mathematics, Royal Holloway, University of London, Egham, Surrey TW20 0EX, UK

E-mail: ville.uski@iki.fi

Received 29 January 2007, in final form 19 April 2007
Published 14 May 2007
Online at stacks.iop.org/JPhysA/40/5857

Abstract

We report on numerical calculations of the distribution of complex Fano parameters in a mesoscopic system consisting of a waveguide attached to a disordered cavity. An external magnetic field in the cavity breaks the time-reversal symmetry. The real and imaginary parts of the parameters as well as the widths are obtained by fitting the Beutler–Fano form to the calculated resonance data. The distributions are compared with the predictions from random matrix theory which have been modified to exclude resonances below a certain cut-off width.

PACS numbers: 05.45.Pq, 72.10.−d, 73.23.−b

1. Introduction

In recent years, there has been much interest in the study of coherent electron transport in mesoscopic systems. Resonances in the scattering cross-section or conductance as a function of energy yield important information about such systems. In particular, the lineshape of the resonance or the so-called Fano q parameter which determines the shape [1, 2] is very sensitive to the interference between the different pathways to the final state of the system and hence to any sources of decoherence.

Fano originally discussed and derived the line shape of a resonance in the context of photoionization spectra, but it has since been studied in many other contexts, such as scattering in atomic and molecular physics, quantum optics, microwave resonators [3], mesoscopic systems [4–6] and other condensed matter systems. The Fano q parameter has mainly been studied for q real. However, recently interest has focussed on situations where q is complex. Kobayashi *et al* [5] showed that in electron transport through a hybrid system consisting of a

[3] Present address: Department of Mathematics, The Open University, Walton Hall, Milton Keynes MK7 6AA, UK.

quantum dot in an Aharonov–Bohm ring the magnetic field breaks the time reversal symmetry (TRS) of the system and the Fano parameter becomes complex. They showed how the real and imaginary parts of q oscillate with the magnetic field giving a variety of line shapes including Lorentzians which normally only occur for real q in the limit $q \to \infty$. Complex q values were also required to interpret the conductance through carbon nanotubes in the presence of a magnetic field [7]. In addition, Rotter *et al* [3] had to introduce complex q parameters to explain the experimental line shapes in microwave transmission through a regular rectangular shaped resonator or cavity. The q parameter is complex due to decoherence from absorption in the walls of the resonator which again leads to a breaking in TRS. They also simulated how decoherence could be introduced by dephasing. In either case complex q values are needed to interpret the results and, in fact, the size of the complex part of q can be used to measure the degree of decoherence present in the system.

In this paper, we analyse the behaviour of complex q parameters for resonances in a chaotic system subject to an external magnetic field which breaks its TRS. In a numerical experiment we simulate a mesoscopic scattering system, composed of an electron moving in a waveguide attached to a disordered cavity in the presence of an external magnetic field. The cavity leads to chaotic motion and hence in addition to being complex the real and imaginary parts of the q parameters should fluctuate randomly. We calculate the conductance as a function of energy and hence by fitting the lineshape of each resonance we extract the real and imaginary parts of the q parameter and the width. We thus obtain the distributions for the real and imaginary parts of q and the widths. We compare our results with the predicted theoretical distributions for a system that obeys random matrix theory (RMT) without TRS [8]. In a recent paper [9], we studied such a system with preserved time-reversal symmetry. Here, we show the corresponding results for the same system but with broken TRS. We find in our simulations, as in any real experiment, that there is an effective cut-off width below which one cannot determine accurately the widths of narrow resonances. This has implications for the RMT predictions where it is assumed that all widths are included. We show how to adapt the RMT predictions to account for this cut-off. When this is done we obtain good agreement between the numerical simulations and the RMT predictions for the distribution of the real and imaginary parts of q and the widths.

The layout of the paper is as follows. In section 2 we outline the numerical method and the model. In section 3 we review the analytical predictions based on the RMT. In section 4 we present the results, and in section 5 we give our conclusions.

2. The model and the calculation of the *S* matrix

We wish to calculate the scattering cross section for an electron moving through a waveguide attached to a chaotic cavity in the presence of a magnetic field. One possible way to achieve this is to have an *irregular* shaped cavity; however, we choose to use a regular shaped cavity and to introduce disorder through the on-site potentials in a tight binding model. This enables one to compute ensemble averages in a straightforward manner by varying the on-site potentials. The system used is illustrated in figure 1.

We approximate the Hamiltonian H of our system with the help of the tight-binding representation:

$$H = \sum_{k} \varepsilon_k c_k^{\dagger} c_k + \sum_{kk'} V_{kk'} c_k^{\dagger} c_{k'}, \tag{1}$$

where the subscripts k denote the sites of a square lattice covering the rectangular cavity and the two-dimensional attached waveguide. $c_k^{\dagger}$ and c_k are the creation and annihilation operators,

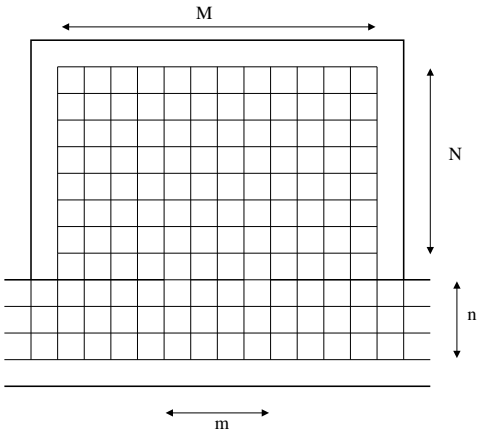

Figure 1. The system is composed of a rectangular cavity with an opening to an infinitely long electron waveguide. The geometry is discretized by a regular square lattice with $m \times n + M \times N$ lattice sites. m is the number of sites connecting the cavity and the waveguide. Each lattice point is associated with an on-site potential ε_k and each connection between the points by a hopping parameter $V_{kk'}$.

corresponding to each site, and ε_k is the potential energy. The hopping parameters $V_{kk'}$ are set equal to the energy unit, if k and k' denote the nearest-neighbour sites. Otherwise $V_{kk'}$ are zero. The on-site potentials ε_k are uniformly distributed in the range $[4 - W/2, 4 + W/2]$ inside the cavity and on the sites across the opening between the cavity and the waveguide, whereas $\varepsilon_k = 4$ elsewhere. W, the disorder strength, is a constant.

To introduce the external magnetic field we apply periodic boundary conditions in the cavity in the horizontal direction (parallel to the waveguide), and multiply those hopping parameters, which connect two adjacent sites in this direction (inside the cavity), by a Peierls phase factor $\exp(\pm 2\pi \mathrm{i}\phi/M)$, where ϕ is the (unitless) magnetic flux and M is the length of the cavity in the units of the lattice spacing [10]. Here, we set $\phi = 1/4$.

For this model we calculate the scattering matrix S as a function of energy with the help of the tight-binding Green function algorithm [11]. The energy range is chosen between the first and second threshold energies of the waveguide, so that S becomes a 2×2 matrix. One sample system is obtained for each set of random on-site potentials, and the S matrix is calculated for a large ensemble of samples. The optical scattering matrix $\bar{S}$ is obtained as the ensemble average of the S matrix, and the parameters q and Γ for each resonance are determined by fitting a Lorentzian profile to the numerical data for the resonant transmission amplitudes $t_r = [S - \bar{S}]_{12}$ (see below). One must be careful to choose the ensemble such that $\bar{S}$ is the same for each sample, which means that the energy interval must be narrow and the on-site potentials in and near the waveguide do not fluctuate from sample to sample (they may fluctuate from site to site, though).

3. Review of RMT theory for the distribution of complex q parameters

In the scattering of a single electron through a waveguide attached to a mesoscopic cavity, Beutler–Fano resonance profiles are seen due to the interference between 'resonant' and 'non-resonant' transmission paths along the waveguide. Here, we assume that the resonant paths enter the cavity and explore it ergodically before re-entering the waveguide. The

non-resonant paths, on the contrary, pass the cavity or enter it for a time shorter than the ergodic time. The transmission amplitude t can be written as a sum of the resonant and non-resonant contributions $t = t_r + t_n$. The resonant contribution t_r is determined by the coupling of the discrete energy levels of a closed cavity and the continuum spectrum of the waveguide [12]. Due to the coupling, the discrete energy levels become resonances and their amplitudes can be represented in a Lorentzian form. The non-resonant contribution t_n is independent of the discrete energy levels of the cavity, and is therefore a slowly varying function of energy. By assuming that it is a constant over the resonance region, one obtains the Beutler–Fano form for the resonance lineshape,

$$g(E) = |t|^2 = |t_n|^2 \frac{|2(E - E_0) + q\Gamma|^2}{4(E - E_0)^2 + \Gamma^2}, \tag{2}$$

where $g(E)$ is the dimensionless conductance, E_0 the resonance position, Γ is the resonance width and q is the Fano parameter.

Γ and q fluctuate according to the statistical properties of the eigenstates of the cavity, which in the ergodic regime follows the predictions of RMT. The distributions are parametrized by the mean level spacing Δ of energy levels belonging to the closed cavity, and the optical scattering matrix $\bar{S}$, which is a sum of the contributions from the direct paths passing the cavity. In the single-channel case considered here, $\bar{S}$ is a subunitary 2×2 matrix, and can be decomposed as follows:

$$\bar{S} = U\sqrt{1 - T}U^{\mathrm{T}}, \tag{3}$$

where U is a 2×2 unitary matrix and $T = \mathrm{diag}(T_1, T_2)$. Equation (3) is known as the Engelbrecht–Weidenmueller transformation [13]. The parameters T_1 and T_2 are called the sticking probabilities [14], and they represent the probability for the electron to enter the ergodic paths from the 'eigenmodes' given by the columns of the matrix U. $\bar{S}$ is here assumed to be symmetric, meaning that the TRS is preserved in the direct (non-resonant) scattering.

In the absence of TRS in the resonant scattering, the Fano parameters are complex. We denote $q = q_1 + \mathrm{i}q_2$, where q_1, q_2 are real. Clerk *et al* [8] derived the distribution for the complex q parameter using RMT. (See [8] for details.) The RMT prediction is

$$P(\tilde{q}_1, \tilde{q}_2) = \frac{1 + \alpha}{2\pi\sqrt{1 - \tilde{q}_1^2 - \tilde{q}_2^2}} \frac{[1 + \alpha(1 - \tilde{q}_1\tilde{q}_a)/2]^2 + \alpha^2\big(1 - \tilde{q}_1^2 - \tilde{q}_2^2\big)\big(1 - \tilde{q}_a^2\big)/4}{\big\{1 + \alpha^2\big[(\tilde{q}_1 - \tilde{q}_a)^2 + \tilde{q}_2^2 - \tilde{q}_2^2\tilde{q}_a^2\big]/4 + \alpha(1 - \tilde{q}_1\tilde{q}_a)\big\}^2} \tag{4}$$

where $\alpha = T_2/T_1 - 1$, $\tilde{q}_1 = q_1/q_1^{\max}$, $q_2 = q_2/q_2^{\max}$, $\tilde{q}_a = q_a/q_1^{\max}$ and $q_1^{\max} = \sqrt{\big(q_2^{\max}\big)^2 - 1}$. The maximum real part is given by $q_1^{\max} = \sqrt{|t_n|^{-2} - 1}$. The parameter q_a is defined as

$$q_a = \mathrm{i}(U_{11}U_{21} - U_{22}U_{12})/(U_{11}U_{21} + U_{22}U_{12}) \tag{5}$$

and is real due to the unitarity of U. Equation (4) applies in the one-channel case, i.e., when there is only one propagating mode in the waveguide.

The distribution of the resonance widths can be deduced from RMT (see [8]), since $\Gamma \propto |\psi|^2$ with a Gaussian random complex ψ, and is given by

$$P(\Gamma) = (\Gamma_1 - \Gamma_2)^{-1}[\exp(-\Gamma/\Gamma_1) - \exp(-\Gamma/\Gamma_2)], \tag{6}$$

where $\Gamma_i = T_i\Delta/2\pi$ for $i = 1, 2$. This formula is valid in the case of isolated resonances.

In real (and numerical) experiments, resonances may be missed for a variety of reasons introducing a bias into the width distributions. In an experiment, absorption can lead to line broadening and to an increase in overlapping resonances which merge with the background or alternatively weak coupling to the measured channel may lead one to miss such weak

resonances. The effect of missing resonances on the statistics of the resonances has been studied recently. Agvaanluvsan *et al* [15] have discussed both how to adapt the Porter–Thomas distribution for the widths when one has to introduce a cut-off for missing widths and how to adapt the nearest neighbour distributions for the positions of the resonances when a fraction of them are missing. Similar studies have been carried out for microwave resonator experiments [16, 17]. In addition, Bohigas and Pato [18] have shown that if the fraction of missing levels is known one can find the statistical properties of the full spectrum or if the statistics of the complete spectrum is known one can find the fraction of missing levels. In our single channel system, by choosing the coupling parameters, we can control many of the possible causes for missing resonances. For example, since the resonance widths Γ are much smaller than the mean-level spacing Δ, overlapping resonances do not play a significant role [8]. The main bias in our width distribution is due to the difficulty in locating all of the very narrow resonances reliably. This 'bias' in sampling will be visible in the q distribution as well, as pointed out in [9]. To simulate the effect of the bias on the RMT statistics, we introduced, as in [15], a simple cut-off $\Gamma_c > 0$ such that $P(\Gamma) = 0$ for all $\Gamma < \Gamma_c$. We then numerically simulated the RMT distribution for the q parameter with a cut-off width distribution by calculating the resonant part of the scattering matrix using wavefunction amplitudes chosen randomly from a normal distribution and excluding those resonances for which $\Gamma < \Gamma_c$. We checked that we recover the theoretical distribution in equation (4) when we choose $\Gamma_c = 0$.

4. Results

We calculated the scattering matrix for the model with the disorder strength $W = 1.0$, $\phi = 0.25$ and energy $E \approx 0.25$ and for a distribution of energies ε_k in equation (1). This energy is near the band edge $E = 0$, so there is only one channel open in the waveguide, i.e., we consider the single-mode case, as in [9]. We take $M = 53$, $N = 20$, $n = 10$, $m = 3$. With these values the statistical properties of the Hamiltonian for the closed cavity follow the predictions of RMT for the Gaussian unitary ensemble, which is the assumption used in applying RMT theory to the open system. For the mean level spacing Δ, we obtained $\Delta \approx 0.01$.

The width Γ and q parameter for a given resonance are calculated as follows. The total phase shift $\delta(E)$ in the vicinity of an isolated resonance can be written as

$$\delta(E) = \arctan\left(\frac{E - E_0}{\frac{1}{2}\Gamma}\right) + \delta_{\mathrm{bg}}(E), \tag{7}$$

where $\delta_{\mathrm{bg}}(E)$ is the background phase shift. The resonance width Γ and position E_0 were determined by fitting this phase shift sum to the numerically determined phase shift, as seen in figure 2 [19].

The transmission amplitude t can be written as

$$t = t_n + t_r = t_n + \frac{z_r \Gamma}{2(E - E_0) + \mathrm{i}\Gamma} \tag{8}$$

where z_r is the excitation amplitude. The Fano parameter is

$$q = \mathrm{i} + z_r / t_n. \tag{9}$$

So by fitting the calculated real and imaginary parts of t as in figure 2, one can extract z_r and hence obtain q.

This is done for 30 000 different realizations of ε_k and the above fitting procedure is implemented for each individual resonance allowing us to calculate the statistical distribution of widths and complex q parameters for our system.

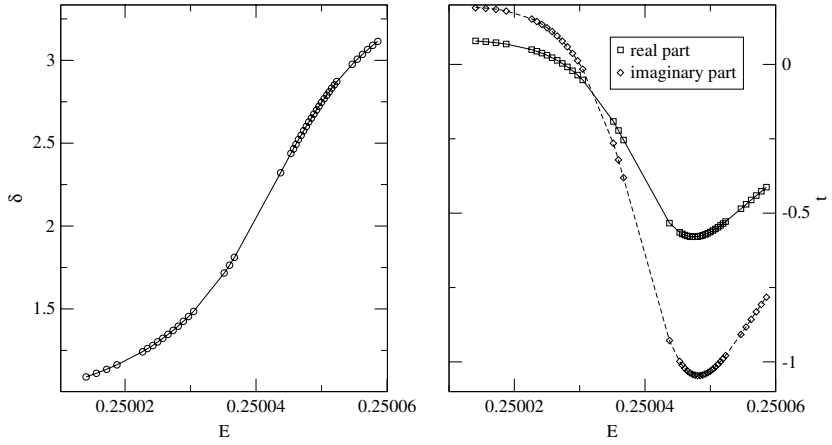

Figure 2. Example resonance. Left: the phase shift as a function of energy (circles) and the fitted Breit–Wigner form. The fit gives the position of the resonance E_0 and the width Γ. Right: real and imaginary parts of the transmission amplitude as a function of energy. The lines show the fit to the data using equation (8). The fit gives the complex Fano parameter q.

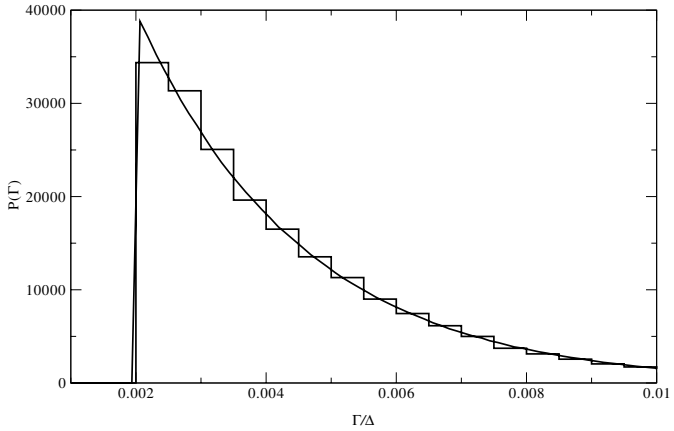

Figure 3. Histogram of the resonance widths. The smooth line shows equation (6) with $\Gamma_1/\Delta = 1.2 \times 10^{-4}$ and $\Gamma_2/\Delta = 2.5 \times 10^{-3}$, a cut-off at $\Gamma/\Delta = 2.0 \times 10^{-3}$ and with a proper renormalization due to the cut-off.

Figure 3 shows the histogram of the obtained resonance widths, compared with the RMT prediction (6). The widths are clearly much smaller than Δ, so it was reasonable to assume that the resonances are isolated. We have cut off the width distribution at $\Gamma_c/\Delta = 2.0 \times 10^{-3}$, where it becomes clear that the narrow widths are under represented. Above this threshold width, there is no statistical error in the resonance searching procedure and the histogram is an excellent agreement with the RMT prediction.

Figure 4 shows separate histograms for the distribution of the real parts and the imaginary parts of the Fano parameter. The numerical data are compared with the RMT prediction (4) both with and without a cut-off. The cut-off reduces the probability of finding large Fano parameters accompanied by an increase in the probability of finding small values. Hence the distributions become more peaked but have their peaks at the same values. The agreement

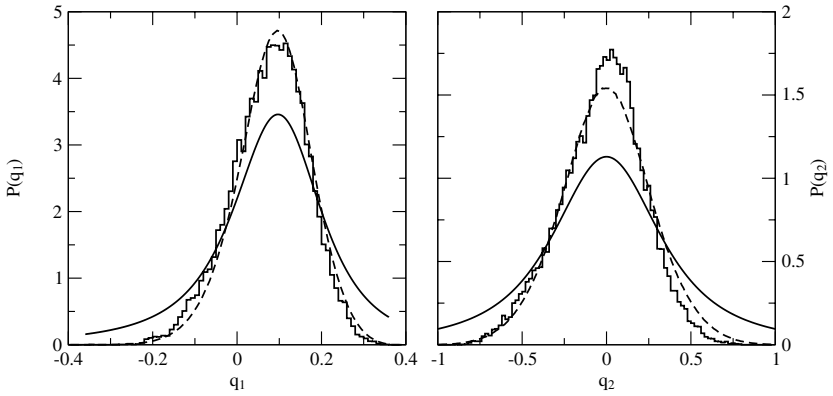

Figure 4. The histograms show the distribution of Fano parameters $P(q_1)$, where q_1 is the real part of q, and $P(q_2)$ with q_2 the imaginary part. The smooth solid lines show the RMT prediction obtained from equation (4) got by integrating out the imaginary and real parts of the full distribution respectively with parameters $\alpha = 20$ and $q_a = 0.094$. The smooth dashed lines show the RMT distributions obtained, when the cut-off at $\Gamma/\Delta = 2.0 \times 10^{-3}$ is taken into account. The histograms have been calculated with the same cut-off.

between the data and the cut-off RMT theory is in general very good for both the real and imaginary parts although the peak in the imaginary part is slightly higher than the predicted value. The RMT theory without a cut-off does not fit the numerical data as is shown in the figure. If we increase the cut-off value we do not find any qualitative difference between the level of agreement between RMT theory and the data. Note that the RMT prediction equation (4) gives a distribution which is symmetric about zero for the distribution of the imaginary parts. However, the simulated data have a slight asymmetry with a lower tail for large positive imaginary parts. This accentuates the differences in the peak values as the distribution has to be normalized. There is a slight shift also between theory and the simulation for the distribution of real parts but this does not have such a pronounced effect on the peak value as the shape of the two distributions is the same. These small differences are understandable in that RMT predictions cannot be found exactly in a finite sample size simulation.

5. Conclusions

We have studied numerically the distribution of widths and complex Fano q parameters for a chaotic scattering system with broken time-reversal symmetry by extracting the widths and q parameters from the calculated phase shifts and transmission amplitudes. We have checked that our model satisfies the main criteria assumed in RMT and we have compared the numerical q histograms for both real and imaginary parts for a system with broken TRS to the theoretical predictions from RMT. The RMT prediction depends on a set of parameters related to the background scattering matrix. These have been determined and very good agreement is obtained between the RMT theory and the calculated distribution when a cut-off is introduced to eliminate resonances with small widths.

References

[1] Fano U 1961 *Phys. Rev.* **124** 1866
[2] Nöckel J U and Stone A D 1994 *Phys. Rev.* B **50** 17415

[3] Rotter S, Kuhl U, Libisch F, Burgdörfer J and Stöckmann H-J 2005 *Physica* E **29** 325
[4] Göres J, Goldhaber-Gordon D, Heemeyer S and Kastner M A 2000 *Phys. Rev.* B **62** 2188
[5] Kobayashi K, Aikawa H, Sano S, Katsumoto S and Iye Y 2004 *Phys. Rev.* B **70** 035319
[6] Johnson A C, Marcus C M, Hanson M P and Gossard A C 2004 *Phys. Rev. Lett.* **93** 106803
[7] Kim J, Kim J-R, Lee J-O, Park J W, So H M, Kim N, Kang K, Yoo K-H and Kim J-J 2003 *Phys. Rev. Lett.* **90** 166403
[8] Clerk A A, Waintal X and Brouwer P W 2001 *Phys. Rev. Lett.* **86** 4636
[9] Uski V, Mota-Furtado F and O'Mahony P F 2005 *J. Phys. A: Math. Gen.* **38** 10819
[10] Luttinger J M 1951 *Phys. Rev.* **84** 814
[11] Sols F, Macucci M, Ravaioli U and Hess K 1989 *J. Appl. Phys.* **66** 3892
[12] Beenakker C W J 1997 *Rev. Mod. Phys.* **69** 731
[13] Engelbrecht C A and Weidenmueller H A 1973 *Phys. Rev.* C **8** 859
[14] Iida S, Weidenmüller H A and Zuk J A 1990 *Ann. Phys., NY* **200** 219
[15] Agvaanluvsan U, Mitchell G E, Shriner J F Jr and Pato M P 2003 *Nucl. Instrum. Methods* A **498** 459
[16] Haake F, Kus M, Seba P, Stöckmann H-J and Stoffregen U 1996 *J. Phys. A: Math. Gen.* **29** 5745
[17] Dembowski C, Dietz B, Friedrich T, Gräf H-D, Harney H L, Heine A, Miski-Oglu M and Richter A 2005 *Phys. Rev.* E **71** 046202
[18] Bohigas O and Pato M P 2004 *Phys. Lett.* B **595** 171
[19] Busby D W, Burke P G, Burke V M, Noble C J and Scott N S 1998 *Comput. Phys. Commun.* **114** 243